Published in final edited form as:
Science. 2014 April 18; 344(6181): 313–319. doi:10.1126/science.1249240.

Enhancing Depression Mechanisms in Midbrain Dopamine Neurons Achieves Homeostatic Resilience

Allyson K. Friedman[1], **Jessica J. Walsh**[1,2], **Barbara Juarez**[1,2], **Stacy M. Ku**[1,2], **Dipesh Chaudhury**[1], **Jing Wang**[3], **Xianting Li**[3], **David M. Dietz**[4], **Nina Pan**[3], **Vincent F. Vialou**[4], **Rachael L. Neve**[5], **Zhenyu Yue**[3,4], and **Ming-Hu Han**[1,4,*]

[1]Department of Pharmacology and Systems Therapeutics, Icahn School of Medicine at Mount Sinai, New York, NY 10029, USA

[2]Neuroscience Program, Graduate School of Biomedical Sciences, Icahn School of Medicine at Mount Sinai, New York, NY 10029, USA

[3]Department of Neurology, Icahn School of Medicine at Mount Sinai, New York, NY 10029, USA

[4]Department of Neuroscience and Friedman Brain Institute, Icahn School of Medicine at Mount Sinai, New York, NY 10029, USA

[5]McGovern Institute for Brain Research, Massachusetts Institute of Technology, Cambridge, MA 02139, USA

Abstract

Typical therapies try to reverse pathogenic mechanisms. Here, we describe treatment effects by enhancing depression-causing mechanisms in ventral tegmental area (VTA) dopamine (DA) neurons. In a social defeat stress model of depression, depressed (susceptible) mice display hyperactivity of VTA DA neurons, caused by an up-regulated hyperpolarization-activated current (I_h). Mice resilient to social defeat stress, however, exhibit stable normal firing of these neurons. Unexpectedly, resilient mice had an even larger I_h, which was observed in parallel with increased potassium (K^+) channel currents. Experimentally enhancing the firing-increasing I_h or optogenetically increasing the hyperactivity of VTA DA neurons in susceptible mice, completely reversed depression-related behaviors, an antidepressant effect achieved through resilience-like, projection-specific homeostatic plasticity. These results indicate a potential therapeutic path of promoting natural resilience for depression treatment.

Resilience is the brain's capacity to cope with environmental stress and achieve stable psychological functioning in response to prolonged stress (1–3). Multiple psychological techniques are used to promote resilience to stress. Specifically, active coping strategies, in which qualities or perceptions of stressors are reassessed, as opposed to avoidant coping, have proven to promote behavioral adaptability and achieve psychological resilience (4, 5). To understand the neurobiological mechanisms underlying stress resilience, tremendous efforts have been made to investigate the genetic, molecular and developmental aspects of

*To whom correspondence should be addressed: Ming-Hu.Han@mssm.edu.

this phenomenon (1, 3, 6, 7). Despite many advances, the neurophysiological processes determining the brain's ability to cope with stress are still poorly understood.

Multiple lines of evidence implicate dysregulation in the brain's reward neural circuit in depression (1, 8–11). In a well-established chronic social defeat model of depression, susceptible and resilient phenotypes have been successfully segregated following a 10-day social defeat paradigm (1, 9, 12, 13). Multiple depressive symptoms in susceptible mice have been causally linked to hyperactivity of ventral tegmental area (VTA) dopamine (DA) neurons (1, 9, 12). Optogenetic activation of these neurons promotes susceptible phenotype, whereas optogenetic reduction of the hyperactivity reverses depression-related behaviors (9). This increase in VTA DA neuron firing in susceptible mice is known to be intrinsically induced by up-regulation of hyperpolarization-activated cation channel-mediated current (I_h), an excitatory driving force in VTA DA neurons (12, 14, 15). Pharmacological reduction of the increased I_h in susceptible mice reverses depression-related symptoms (12). Chronic antidepressant fluoxetine treatment normalizes the hyperactivity and decreases I_h in these neurons (12). These observations suggest that hyperactivity and increased excitatory I_h in VTA DA neurons are both pathophysiological adaptations underlying the susceptible phenotype.

To understand the neurophysiological mechanisms of the resilient phenotype following chronic social stress, we employed tyrosine-hydroxylase (TH)-GFP mice to visualize and reliably record from VTA DA neurons (fig. S1A). TH-GFP mice that undergo chronic social defeat stress reliably separate into either susceptible or resilient phenotypes based on social interaction ratios (fig. S1, B and C) (1, 9, 12, 13). Susceptible TH-GFP mice showed social avoidance, spending significantly less time in the interaction zone, while resilient mice spent a significant amount of time with the social target, similar to that of control mice (fig. S1, D to G). Susceptible mice also display other depression-related anhedonic behaviors (fig. S1H) (1, 7). We confirmed pathophysiological hyperactivity in the GFP-visualized DA neurons of susceptible TH-GFP mice (fig. S1I), while the pacemaker firing pattern was the same in the three groups. Overall, the resilient TH-GFP mice exhibited a stable control level firing of VTA DA neurons, appearing not to have undergone any pathogenic changes at cellular and behavioral levels in response to chronic social defeat stress (fig. S1, D to I and fig. S2).

We next investigated if the pathophysiological increase in I_h current is normalized in resilient mice. We performed whole-cell voltage-clamp recordings in GFP^+ VTA DA neurons in brain slices from control, susceptible and resilient TH-GFP mice. In accordance with previous findings (12), I_h was increased in susceptible mice (Fig. 1A). However, unexpectedly, rather than a normalization of the I_h levels in resilient mice, the resilient phenotype showed an even larger significant increase in I_h when compared to susceptible and control mice (Fig. 1A). This was surprising and unanticipated because this firing-increasing I_h was viewed as a stress-induced, pathological ion mechanism in susceptible mice.

To understand how VTA DA neurons in resilient mice maintain a level of firing similar to control mice with this extremely larger I_h, we focused on K^+ channels, an inhibitory driving force that was up-regulated selectively in the resilient subgroup in a previous microarray

analysis (1). The VTA DA neurons of resilient mice, which displayed a further enhanced I_h, simultaneously exhibited significantly increased K^+ channel-mediated peak and sustained currents (Fig. 1B), implicating multiple K^+ channel types mediating this increase in K^+ currents.

To investigate a possible benefit of resilient mice recruiting these extra channel functions, we measured intrinsic excitabilities of VTA DA neurons in the three groups. In response to a series of current injections, we observed an increase in spike number in susceptible mice, and inversely, a reduction in spike number in resilient mice, as compared to control mice (Fig. 1C). This suggests that the re-established status of VTA DA neurons in resilient mice is more stable and less vulnerable to perturbations than that of control.

The up-regulation of I_h in VTA DA neurons of resilient mice may be driving the neuronal firing extremely high and triggering a self-tuning K^+ current mechanism to bring the extreme firing back to control (fig. S3). This in turn normalizes the depressive behaviors. To determine whether enhancing I_h current in susceptible mice can trigger this hypothesized homeostatic plasticity observed in the resilient mice, we pharmacologically increased I_h through *in vivo* infusion of an I_h potentiator, lamotrigine, into the VTA of TH-GFP susceptible mice. Lamotrigine is known to enhance I_h (16) and is clinically used as a mood stabilizer to treat the depressed phase of bipolar disorder with uncertain mechanisms (17). In brain slices, bath application of lamotrigine increased I_h and the firing rate of VTA DA neurons (fig. S4). Consistently, a single *in vivo* infusion into the VTA of susceptible mice increased social avoidance (fig. S5). To determine if repeated enhancement of this current can induce a homeostatic compensatory response, we performed repeated 5 day local infusions of lamotrigine (0.1 μg) into the VTA of susceptible TH-GFP mice because it is known that 4–5 days is sufficient to induce stable changes in social behaviors (Fig. 1, D and E, and fig. S6A) (18). After 5 days of local infusion, we observed a profound reversal of social avoidance, with more time spent interacting with a social target (Fig. 1F) and reduced time in the corner zone (fig. S6B), without adverse effects on locomotion (fig. S6C). The defeat-induced deficit in sucrose preference was also significantly reversed following repeated lamotrigine infusion (Fig. 1G), indicating an overall resilient, antidepressant effect, without affecting the behaviors in either control or resilient mice (fig. S7 and S8).

Consistent with the behavioral antidepressant effect, the hyperactivity of VTA DA neurons in susceptible mice was normalized following I_h potentiation via lamotrigine (Fig. 1H). To examine the ionic mechanisms that underlie this promotion of resilience, we determined the effects of repeated lamotrigine infusion on I_h and K^+ currents. We observed a marked increase in I_h (Fig. 1I) and a compensatory increase in K^+ currents (Fig. 1J), a phenomenon not observed at lower doses (fig. S9). Consistently, these ionic changes induced a reduction in DA neuron excitability in the lamotrigine treated animals (Fig. 1K) as compared to vehicle control. These data describe a possible mechanism of lamotrigine's mood stabilizing efficacy.

While one of the actions of lamotrigine is known to increase I_h current, lamotrigine has other effects on neurons such as blockade of sodium channels (19). To specifically assess the role enhanced I_h has in VTA DA neurons, we selectively over-expressed

hyperpolarization-activated and cyclic nucleotide-gated channel 2 (HCN2), a channel isoform which mediates I_h current (20). We used a combination of TH-Cre mice and Cre-inducible loxP-STOP-loxP herpes simplex virus (HSV-LS1L-HCN2-eYFP), and HSV-LS1L-eYFP as control. The HSV vectors allow for the rapid expression of HCN2 over 5 days (18). The Cre-inducible vectors were injected bilaterally into the VTA of TH-Cre transgenic mice to ensure specific expression in DA neurons (Fig. 2, A and B). Functional validation 24 hours post injection successfully showed an increase in I_h (Fig. 2C) and corresponding increase in firing (Fig. 2D). Next, we injected HSV-LS1L-HCN2-eYFP or HSV-LS1L-eYFP into the VTA of susceptible TH-Cre mice and carried out the behavioral and electrophysiological measurements 4–6 days after viral injection (Fig. 2, E and F). Over-expression of HCN2 in the VTA DA neurons of susceptible mice resulted in a reversal of social avoidance (Fig. 2G and fig. S10A) and other depressive behaviors (Fig. 2, H and I) with no affect on locomotion (fig. S10B).

Following DA neuron-specific expression of HCN2 in susceptible mice, a robust reduction in hyperactivity was found in HCN2 expressing DA neurons, as compared to eYFP control (Fig. 2J). We observed a significant increase in I_h current in HCN2-expressing cells (Fig. 2K) and in conjunction, we observed a significant increase in the K^+ currents (Fig. 2L), resulting in an overall reduction in excitability of these neurons (Fig. 2M).

While excessively potentiating I_h resulted in a homeostatic up-regulation of K^+ channel function in VTA DA neurons of susceptible mice, this K^+ current compensation may be caused directly by the hyperactivity induced by I_h potentiation. In primary neuronal cultures excessive hyperactivity can induce homeostatic up-regulation of K^+ channel-mediated current (21). We thus asked whether direct excessive activation of VTA DA neurons in susceptible mice could induce a functional K^+ channel counteraction that would normalize the hyperactivity of these neurons and depression-related behaviors. We examined social interaction behaviors and the channel functions following repeated optogenetic activation of VTA DA neurons in susceptible mice – further increasing the hyperactivity in susceptible mice. We injected Cre-inducible adenovirus-associated channelrhodopsin-2 (AAV-DIO-ChR2-eYFP) or control vector (AAV-DIO-eYFP) into the VTA of susceptible TH-Cre mice to selectively express ChR2 in VTA DA neurons (Fig. 3, A to C) (9, 22, 23). Bilateral implantable optic fibers were placed above the VTA (fig. S11A) for blue light photo-stimulation (5 pulses, 20 Hz/10 sec period; Fig. 3, D and E) of DA neurons in susceptible mice, mimicking a validated *in vivo* firing pattern (9, 12, 23, 24). After 5 days of 20 min photo-stimulation, susceptible mice with viral expression of ChR2 showed reduced social avoidance, (Fig. 3F and fig. S11B) and reduced depressive behaviors (Fig. 3, G and H), without adverse effects on locomotion (fig. S11C). Excessive optogenetic activation of VTA DA neurons in susceptible mice reduced firing rate (Fig. 3I) and increased K^+ currents (Fig. 3J) in the ChR2-infected neurons, without altering I_h (fig. S11D). Consistent with the ionic alterations, we found a reduction in excitability of the ChR2-infected neurons (Fig. 3K).

Recent studies show that VTA DA neurons are heterogeneous (9, 11, 25, 26). For instance, VTA DA neurons projecting to nucleus accumbens (NAc) exhibit a large I_h, while medial prefrontal cortex (mPFC)-projecting VTA DA neurons have a small I_h (26). Utilizing retrograde tracers, we found that I_h alterations in response to chronic social defeat occur

specifically in NAc-projecting VTA neurons, but not in mPFC-projecting VTA neurons (Fig. 4A and 4H, and fig. S12A and S13A). Interestingly, the homeostatic plasticity that occurs in response to projection-specific HCN2 over-expression and repeated optogenetic stimulation is unique to the VTA-NAc projection (Fig. 4, B to G, and fig. S12). A different form of plasticity occurred in VTA-mPFC neurons: surprisingly, HCN2 over-expression had no effects on behavior, firing, $I_{h,}$ and K^+ currents (Fig. 4, I to K, and fig. S13, B to G), whereas repeated optogenetic stimulation reversed social avoidance accompanied by a firing increase and a K^+ current decrease, the physiological changes opposite to what were seen in VTA-NAc neurons (Fig. 4, L to N, and fig. S13, H to L).

Self-tuning adaptation of neuronal activity as a homeostatic plasticity concept was first described in primary neuronal culture (27) and further observed in *in vivo* animal models (28, 29). Evidence demonstrates that homeostatic plasticity plays a fundamental role in stabilizing neuronal activity in response to excessive perturbations under both physiological (30, 31) and disease (32) conditions. We observed that resilient mice displayed enhanced I_h current in VTA DA neurons, and simultaneously exhibited up-regulated inhibitory K^+ currents. Based on this unexpected observation, we tested the hypothesis that the resilience phenotype achieves its stable behavioral functioning through homeostatic plasticity and that this homeostatic adaptation can be established therapeutically in susceptible mice. Utilizing pharmacological, viral and optogenetic approaches, we found that enhancement of I_h or excessive activation of VTA DA neurons triggered self-tuning compensation of K^+ currents and functionally normalized the firing of these hyperactive neurons in susceptible animals, a homeostatic plasticity seen in VTA-NAc projection, but not in VTA-mPFC pathway. Once the homeostatic balance is established naturally or experimentally in VTA DA neurons, these neurons are more stable as indicated by their reduced response to physiological perturbation. Our findings advance the understanding of homeostatic plasticity in a behaviorally relevant *in vivo* disease model of depression and provide further insight into the stabilized physiological underpinnings of natural resilience.

While homeostatic plasticity describes much of our current findings, the counterintuitive process by which ionic, cellular and behavioral alterations are achieved and its close similarity to natural stress-resilience remains surprising. Recently, cell type-specific and neural circuit-probing optogenetic approaches has assisted in unraveling multiple unforeseen functions of the brain's reward DA neurons (9, 11, 22, 23, 26, 33). By revealing a previously uncharacterized ionic mechanism of intrinsic homeostatic plasticity we are bringing new insight to the complex functions of these neurons. Notably, the experimentally induced homeostatic plasticity in VTA-NAc projecting neurons is triggered by enhancing stress-activated I_h current and stress-induced neuronal hyperactivity. Therefore, rather than reversing the underlying disruption or pathological mechanisms the stress-activated pathogenic changes can be beneficially used to achieve treatment efficacy (fig. S14). Interestingly, reversing pathological adaptations rapidly induces antidepressant effects (9, 11), while chronic manipulations are needed to promote active resilient mechanisms and achieve treatment efficacy. Overall, our findings not only unravel a critical self-stabilizing capacity of midbrain DA neurons in the brain's reward circuit, but also identify a

conceptually different therapeutic strategy of promoting natural resilience. This may provide useful information for the development of naturally acting antidepressants.

Supplementary Material

Refer to Web version on PubMed Central for supplementary material.

Acknowledgments

We thank E.J. Nestler for his continuing support of this work. We also thank S.J. Russo, H.P. Xu, J.L. Cao, F. Henn, and E.J. Nestler for their helpful discussion. We are grateful to G.R. Tibbs and P.A. Goldstein from Weill Cornell Medical College for providing the HCN2 plasmid. This work was supported by the National Institute of Mental Health (R01 MH092306: S.M.K., D.C., M.H.H.), National Research Service Award (F31 MH095425: J.J.W.; T32 MH 087004: B.J.; F32 MH096464: A.K.F.), and Johnson & Johnson/IMHRO Rising Star Translational Research Award (M.H.H.).

References and Notes

1. Krishnan V, et al. Cell. 2007; 131:391. [PubMed: 17956738]
2. Feder A, Nestler EJ, Charney DS. Nat Rev Neurosci. 2009; 10:446. [PubMed: 19455174]
3. Russo SJ, Murrough JW, Han MH, Charney DS, Nestler EJ. Nat Neurosci. 2012; 15:1475. [PubMed: 23064380]
4. Kumar S, Feldman G, Hayes A. Cognitive Therapy and Research. 2008; 32:734.
5. Carey TA. Clinical Psychology Review. 2011; 31:236. [PubMed: 20447745]
6. Southwick SM, Charney DS. Science. 2012; 338:79. [PubMed: 23042887]
7. Vialou V, et al. Nat Neurosci. 2010; 13:745. [PubMed: 20473292]
8. Nestler EJ, Carlezon WA Jr. Biol Psychiatry. 2006; 59:1151. [PubMed: 16566899]
9. Chaudhury D, et al. Nature. 2012
10. Berton O, et al. Science. 2006; 311:864. [PubMed: 16469931]
11. Tye KM, et al. Nature. 2013; 493:537. [PubMed: 23235822]
12. Cao JL, et al. The Journal of Neuroscience. 2010; 30:16453. [PubMed: 21147984]
13. Golden SA, Covington HE, Berton O, Russo SJ. Nat Protocols. 2011; 6:1183.
14. Wanat MJ, Hopf FW, Stuber GD, Phillips PEM, Bonci A. The Journal of Physiology. 2008; 586:2157. [PubMed: 18308824]
15. Neuhoff H, Neu A, Liss B, Roeper J. J Neurosci. 2002; 22:1290. [PubMed: 11850457]
16. Poolos NP, Migliore M, Johnston D. Nat Neurosci. 2002; 5:767. [PubMed: 12118259]
17. Frye MA. New England Journal of Medicine. 2011; 364:51. [PubMed: 21208108]
18. Wilkinson MB, et al. The Journal of Neuroscience. 2011; 31:9084. [PubMed: 21697359]
19. Nakatani Y, Masuko H, Amano T. Journal of Pharmacological Sciences. 2013; 123:203. [PubMed: 24096830]
20. Biel M, Wahl-Schott C, Michalakis S, Zong X. Physiol Rev. 2009; 89:847. [PubMed: 19584315]
21. Zhang J, Shapiro MS. Neuron. 2012; 76:1133. [PubMed: 23259949]
22. Tsai HC, et al. Science. 2009; 324:1080. [PubMed: 19389999]
23. Walsh JJ, et al. Nature Neuroscience. 2014; 17:27.
24. Koo JW, et al. Science. 2012; 338:124. [PubMed: 23042896]
25. Margolis EB, Mitchell JM, Ishikawa J, Hjelmstad GO, Fields HL. J Neurosci. 2008; 28:8908. [PubMed: 18768684]
26. Lammel S, et al. Neuron. 2008; 57:760. [PubMed: 18341995]
27. Turrigiano G, Abbott LF, Marder E. Science. 1994; 264:974. [PubMed: 8178157]
28. Turrigiano G. Annu Rev Neurosci. 2011; 34:89. [PubMed: 21438687]
29. Maffei A, Nataraj K, Nelson SB, Turrigiano GG. Nature. 2006; 443:81. [PubMed: 16929304]

30. Destexhe A, Marder E. Nature. 2004; 431:789. [PubMed: 15483600]
31. Whalley K. Nat Rev Neurosci. 2013; 14:820. [PubMed: 24201182]
32. Dickman DK, Davis GW. Science. 2009; 326:1127. [PubMed: 19965435]
33. Lammel S, et al. Nature. 2013; 491:212. [PubMed: 23064228]
34. Wallace DL, et al. Nat Neurosci. 2009; 12:200. [PubMed: 19151710]

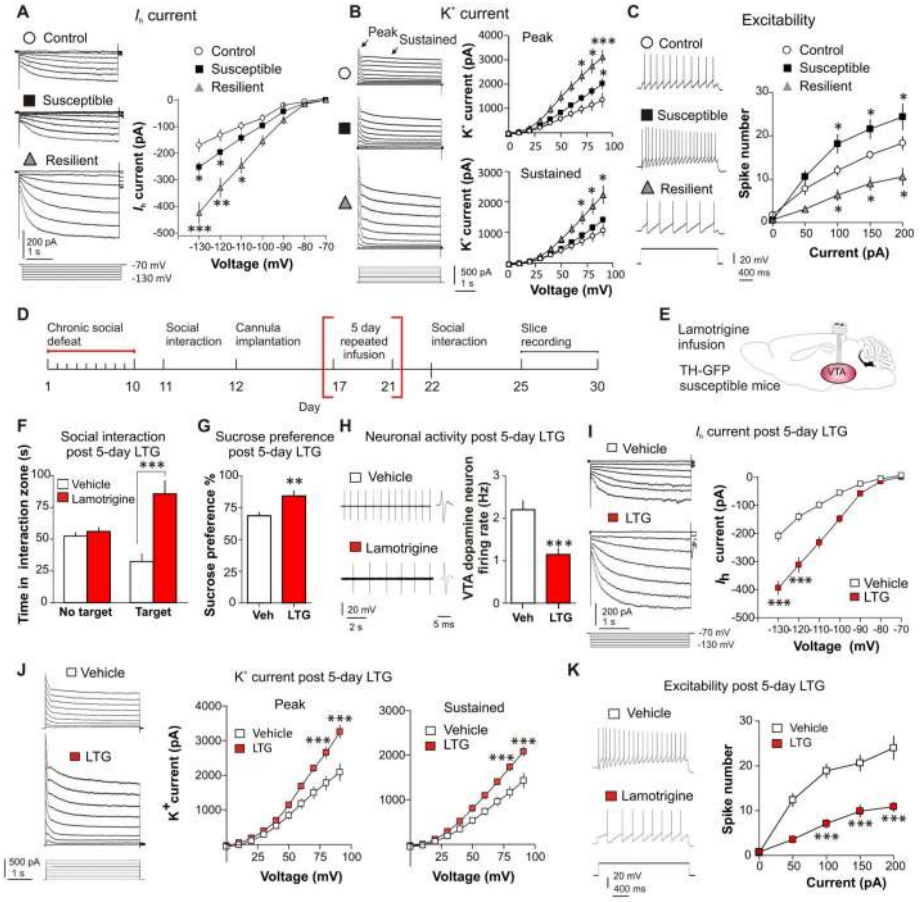

Fig. 1.

The resilient phenotype shows dramatically increased I_h and K^+ channel currents in VTA DA neurons, and repeated infusion of I_h potentiator lamotrigine to the VTA of susceptible mice achieves antidepressant effects by inducing similar homeostatic plasticity. (**A**) Hyperpolarization-activated cation channel-mediated current (I_h) sample traces and statistic data for control (○), susceptible (■) and resilient (▲) mice. At −130 mV, $F_{(2,47)} = 19.19$, $P < 0.0001$; At −120 mV, $F_{(2,62)} = 17.69$, $P < 0.001$; n = 12–22 cells/8–10 mice per group. Post hoc at −130 mV analysis shows a significant increase in I_h in susceptible mice ($t_{32} = 2.65$, $P < 0.05$) and, an even significantly larger I_h increase in the resilient subgroup ($t_{24} = 5.24$, $P < 0.001$), compared to control. (**B**) Sample traces and statistic data of isolated K^+ channel-mediated currents recorded from VTA DA neurons show resilient mice have significantly increased peak and sustained phases of K^+ currents. At +90 mV, $F_{(2,58)} = 15.129$, $P < 0.001$; n = 14–23 cells/9–10 mice per group. Post hoc analysis shows a slight increase in peak K^+ currents in susceptible mice ($t_{41} = 2.62$, $P < 0.05$) and a larger increase in the resilient subgroup ($t_{36} = 5.25$, $P < 0.001$), compared to control. (**C**) Susceptible mice display increased DA neuron excitability while resilient mice display a reduction, following incremental steps in current injections (50, 100, 150, and 200 pA) compared to controls (at 100 pA: $F_{(2,28)} = 12.00$, $P < 0.001$; at 150 pA $F_{(2,28)} = 12.66$, $P < 0.001$ and at 200 pA $F_{(2,25)} = 8.86$, $P < 0.001$). Post hoc analysis of susceptible and resilient compared to control for 100 and 150 and 200 pA currents at $P < 0.05$ (n = 8–12 cells/7–8 mice per group). (**D**

and **E**) Experimental timeline and schematic. (**F**) 5 day 4 min daily bilateral infusions of lamotrigine (LTG, 0.1 μg) or vehicle into the VTA reversed social avoidance ($t_{18} = 5.79$, $P < 0.001$; n = 10) and (**G**) sucrose preference ($t_{18} = 3.25$, $P < 0.01$; n = 10). (**H)** Sample traces and statistic data of VTA DA neuron firing in susceptible mice following repeated infusion of vehicle compared to lamotrigine ($t_{32} = 4.10$, $P < 0.001$; n = 17 cells/7–9 mice per group). (**I**) Sample traces and statistic data of I_h in susceptible mice following repeated infusion of vehicle (□) or lamotrigine (■) (at −130 mV: $t_{13} = 6.99$, $P < 0.0001$; at −120 mV: $t_{13} = 5.88$, $P < 0.0001$; n = 7–8 cells/6–8 mice per group). (**J)** Sample traces and statistic data of K^+ currents in susceptible mice following repeated infusion of vehicle or lamotrigine: Peak (at +20 mV: $t_{19} = 5.03$, $P < 0.001$; at +10 mV: $t_{19} = 5.92$, $P < 0.001$) and sustained (at +20 mV: $t_{19} = 5.95$, $P < 0.001$; at +10 mV: $t_{19} = 6.81$, $P < 0.001$; n = 10–11 cells/7–9 mice per group). (**K**) Sample traces obtained at 100 pA current injection and statistic data of decreased excitability in susceptible mice infused with lamotrigine compared to vehicle (at 100 pA: $t_{15} = 6.41$, $P < 0.0001$; at 150 pA: $t_{15} = 4.93$, $P < 0.001$; at 200 pA: $t_{15} = 4.56$, $P < 0.001$; n = 8–9 cells/7–9 mice per group). Error bars, ± s.e.m. * $P < 0.05$, ** $P < 0.01$, *** $P < 0.001$.

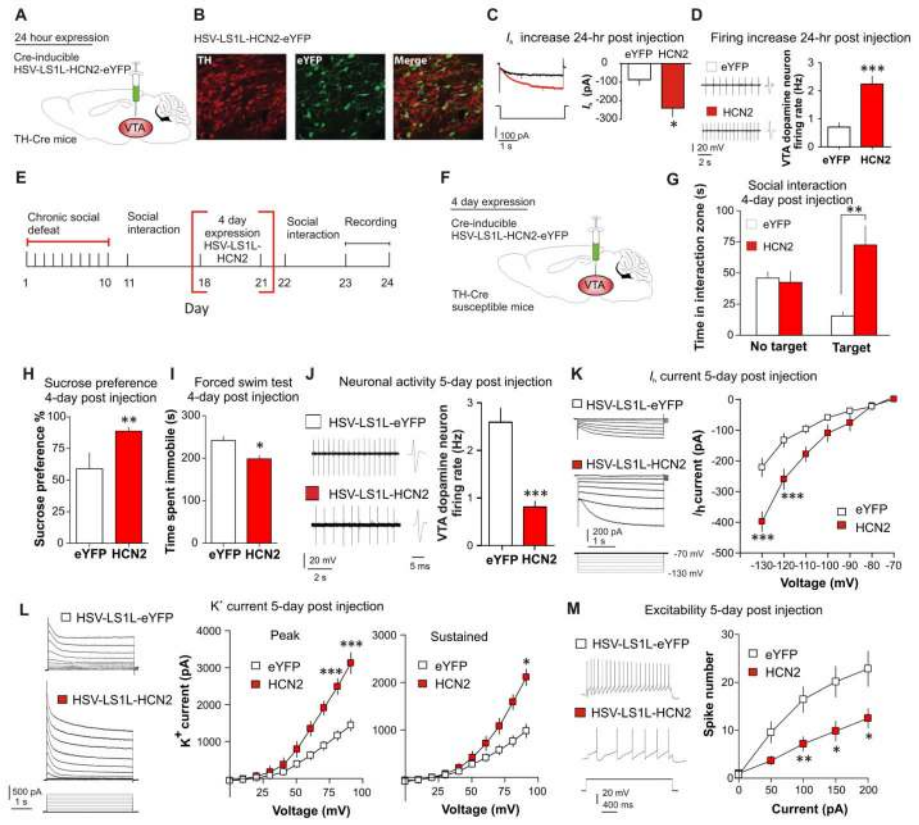

Fig. 2.

DA neuron-specific overexpression of HCN2 channel induces an antidepressant behavioral effect and triggers a homeostatic response via an increase in compensatory K^+ currents. (**A**) Cre-inducible HSV-LS1L-HCN2-eYFP injection into the VTA of TH-Cre mice. (**B**) Confocal image showing colocalization (merge) of Cre-induced HCN2 (eYFP) expression in VTA DA neurons (TH) of TH-Cre mice. Quantification shows that HCN2-expressing TH^+ cells were 47±4% of total TH^+ neurons in the VTA and there was no expression of HCN2 in TH^- neurons (2–3 sections per mouse; n = 4). Scale bar 100 μm; green, eYFP; red, TH. (**C**) Virally expressed HCN2 significantly increases I_h ($t_{13} = 2.73$, $P < 0.05$; n = 7–8cells/group, 3 mice/group) and (**D**) firing rate ($t_{25} = 6.86$, $P < 0.0001$; n = 13–14 cells/4 mice/group) in VTA DA neurons as compared to control (eYFP) 24 hours post injection. (**E** and **F**) Experimental timeline and schematic. Behavioral effects of susceptible mice expressing HSV-LS1L-HCN2-eYFP or control HSV-LS1L-eYFP in DA neurons of the VTA on (**G**) social interaction test ($t_{22} = 3.72$, $P < 0.01$; n = 12), (**H**) sucrose preference test ($t_{18} = 3.40$, $P < 0.01$; n = 10) and (**I**) immobility time during forced swim test ($t_{18} = 2.87$, $P < 0.05$; n = 10). (**J** to **L**) Neuronal effects of 6 days of expression of HSV-LS1L-HCN2-eYFP (■) compared to HSV-LS1L-eYFP (□) in DA neurons of the VTA in susceptible mice on (**J**) firing rate ($t_{19} = 5.48$, $P < 0.0001$; n = 10–11), (**K**) I_h measurements (at −130 mV: $t_{22} = 4.51$, $P < 0.001$; at −120 mV: $t_{18} = 3.25$, $P < 0.005$) and (**L**) K^+ currents (−70 mV to +20 mV/10 mV step): Peak (at +20 mV: $t_{16} = 5.70$, $P < 0.001$; at +10 mV: $t_{16} = 5.28$, $P < 0.001$), sustained (at +20 mV: $t_{16} = 2.480$, $P < 0.05$). (**M**) Sample traces at 100 pA current injection and statistic data of decreased excitability in susceptible mice expressing HCN2 compared

to eYFP control (at 100 pA: $t_{12} = 3.21$, $P < 0.01$; at 150 pA: $t_{12} = 2.73$, $P < 0.05$; at 200 pA: $t_{12} = 2.54$, $P < 0.05$; n = 7 cells/6–7 mice per group). Error bars, ± s.e.m. * $P < 0.05$, ** $P < 0.01$, *** $P < 0.001$.

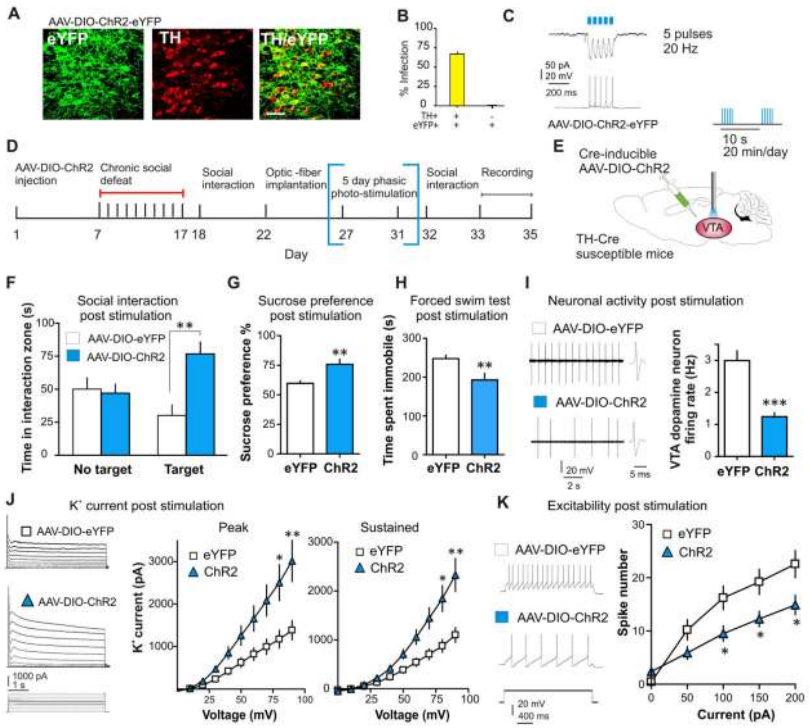

Fig. 3.

Repeated optogenetic stimulation of VTA DA neurons normalizes the depressed phenotype and induces a significant compensation in K^+ currents. (**A**) Cell type-specific AAV-DIO-ChR2-eYFP expression (green) in VTA DA neurons (red) of TH-Cre mice. Scale bar 100 μm. **(B)** Quantification shows that ChR2-expressing TH^+ cells are 67±4% of total TH^+ neurons in the VTA and there was no expression of ChR2 in TH^- neurons (n = 2–3 sections per mouse; n = 5 animals). **(C)** Voltage-clamp (upper trace) and current-clamp (lower trace) recordings from DA neurons in VTA slices. Five short bursts (20 Hz, 40 ms) of blue light (470 nm) induce temporally precise inward photocurrents and corresponding action potentials. (**D**) Experimental timeline (**E**) Localization of bilateral viral injection and optic-fiber implantation used for *in vivo* delivery of blue light in susceptible TH-Cre mice. 470-nm phasic light pulses (20 Hz, five pulses/10 sec) were delivered 20 min a day for 5 consecutive days. (**F**) After 5 days (20 min/day) of phasic stimulation of DA neurons, susceptible animals expressing ChR2 have increased social interaction ($t_{22} = 3.59$, $P < 0.01$; n = 12), (**G**) increased sucrose preference ($t_{20} = 3.25$, $P < 0.01$; n = 11), and (**H**) decreased immobility time during forced swim test ($t_{18} = 2.89$, $P < 0.01$; n = 10). (**I**) Sample traces and statistic data of VTA DA neuron firing in susceptible mice following chronic excessive activation ($t_{23} = 6.25$, $P < 0.001$; 12–13 cells/6 mice per group). (**J**) Sample traces and statistic data of K^+ currents recorded from VTA DA neurons in brain slices from eYFP and ChR2-expressing neurons. Excessive optical activation of VTA DA neurons significantly increased the peak (at +20 mV: $t_{19} = 3.08$, $P < 0.01$; at +10 mV: $t_{19} = 2.83$, $P < 0.05$; at 0 mV) and sustained (at +20 mV: $t_{19} = 3.53$, $P < 0.01$; +10 mV: $t_{19} = 3.18$, $P < 0.05$) phases of K^+ currents. (**K**) Sample traces at 100 pA current injection and statistic data of decreased excitability in susceptible mice expressing ChR2 compared to eYFP (at 100 pA: $t_{15} = 2.47$,

$P < 0.05$; at 150pA: $t_{15} = 2.41$, $P < 0.05$; at 200pA: $t_{15} = 2.32$, $P < 0.05$; n = 8–9 cells/6–8 mice per group). Error bars, ± s.e.m. * $P < 0.05$, ** $P < 0.01$, *** $P < 0.001$.

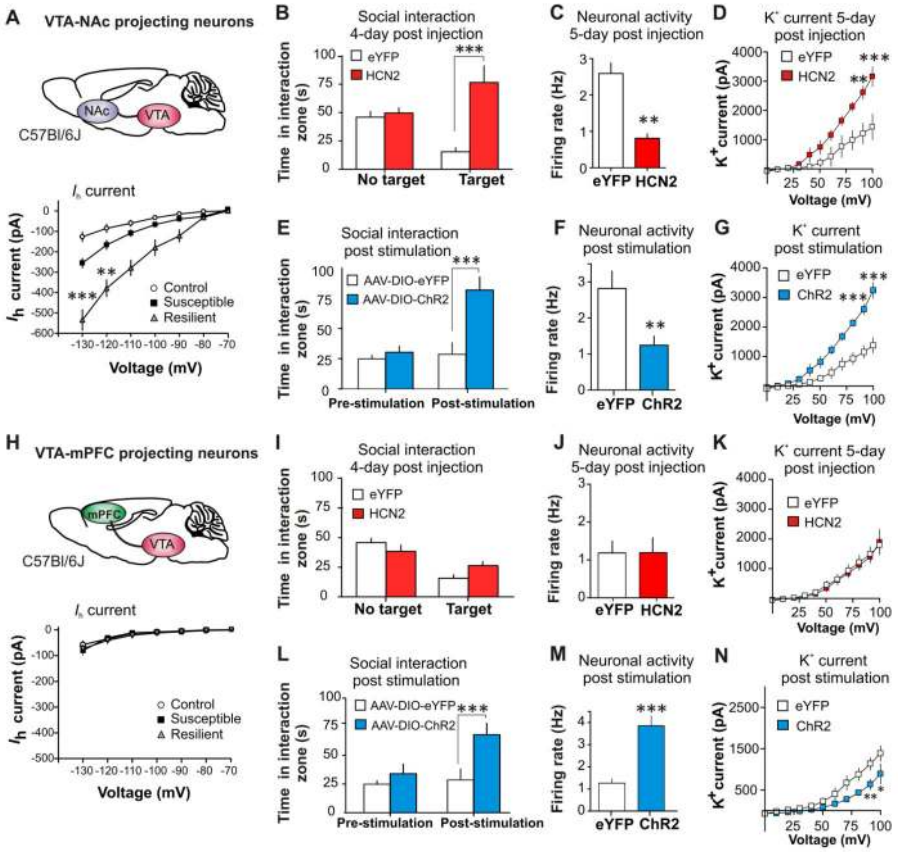

Fig. 4.

The observed homeostatic plasticity is specific in the I_h-presenting VTA-NAc projection. (**A**) Statistics data of I_h in NAc projecting VTA (VTA-NAc) neurons in control, susceptible and resilient mice. At −130 mV, $F_{(2,22)} = 39.27$, $P < 0.0001$; At −120 mV, $F_{(2,22)} = 27.78$, $P < 0.0001$; n = 7–10 cells/6–7 mice per group. Post hoc analysis at −130 shows a significant increase in I_h in susceptible mice ($t_{16} = 3.98$, $P < 0.01$) and, an even significantly larger I_h increase in the resilient subgroup ($t_{13} = 7.71$, $P < 0.001$), compared to control. (**B**) Susceptible mice expressing HCN2 in VTA-NAc neurons show an increase in social interaction ($t_{13} = 4.81$, $P < 0.001$; n = 7–8) and (**C**) a decrease in the firing rate of VTA-NAc neurons ($t_{22} = 3.31$, $P < 0.01$; n = 11–13 cells/6 mice per group) compared to eYFP. (**D**) K^+ currents: Peak (at +20 mV: $t_{12} = 4.47$, $P < 0.001$; at +10 mV: $t_{12} = 4.33$, $P < 0.01$; n = 7 cells/6 mice per group). (**E**) After 5 days (20 min/day) of optical phasic stimulation of VTA-NAc neurons, susceptible animals expressing ChR2 have increased social interaction ($t_{18} = 4.24$, $P < 0.001$, n = 10) and (**F**) a decrease in the firing of VTA-NAc neurons expressing ChR2 ($t_{19} = 3.44$, $P < 0.01$, n = 10–11 cell/5–6 mice per group). (**G**) K^+ currents are significantly increased in ChR2 expressing neurons: Peak (at +20 mV: $t_{12} = 4.70$, $P < 0.001$; at +10 mV: $t_{12} = 4.82$, $P < 0.001$; n = 7 cells/6 mice per group). (**H**) Statistics data of I_h in mPFC projecting VTA (VTA-mPFC) neurons in control, susceptible and resilient mice. At −130 mV, ($F_{(2,38)} = 0.69$, $P = 0.51$; n = 9–11 cells/5–6 mice per group. Susceptible mice expressing HCN2 or control eYFP in VTA-mPFC show no change in (**I**) social interaction ($t_{18} = 1.65$, $P = 0.12$; n = 10), (**J**) firing rate of VTA-mPFC neurons ($t_{24} = 0.34$, $P = 0.74$; n

= 13 cells/group 5–6 mice per group) and (**K**) no change in K^+ currents of VTA-mPFC neurons: Peak (at +20 mV: $t_{14} = 0.12$, $P = 0.90$; at +10 mV: $t_{14} = 0.85$, $P = 0.41$; n = 8 cells/6 mice per group). After 5 days (20 min/day) of optical phasic stimulation of VTA-mPFC neurons, susceptible animals expressing ChR2 have increased (**L**) social interaction ($t_{18} = 4.07$, $P < 0.001$, n = 10) and (**M**) an increase in the firing of VTA-mPFC neurons ($t_{24} = 5.11$, $P < 0.0001$, n = 12–14 cell/group 6 mice per group). (**N**) K^+ currents are significantly decreased following chronic activation: Peak (at +20 mV: $t_{14} = 2.26$, $P < 0.05$; at +10 mV: $t_{14} = 3.20$, $P < 0.01$; n = 8 cells/6 mice per group). Error bars, ± s.e.m. * $P < 0.05$, ** $P < 0.01$, *** $P < 0.001$.